Research and Development of Multi-axis CNC Abrasive Belt-Grinding Machine Postprocessor

Hu Qiao
Xi'an Technological University
Zhenxing Wei (1922271857@qq.com)
Xi'an Technological University https://orcid.org/0000-0002-7167-5836
Ruixiang Deng
Xi'an Technological University
Tianhang Xu
Xi'an Technological University
Ying Xiang
Shaanxi University of Science and Technology

Research Article

Keywords: CNC Abrasive Belt-Grinding Machine, Geometric Modeling, Postprocess, Virtual simulation, Hollow Blade

Posted Date: May 24th, 2022

DOI: https://doi.org/10.21203/rs.3.rs-1631777/v1

Research and Development of Multi-axis CNC Abrasive Belt-Grinding Machine Postprocessor

Hu Qiao[1], Zhenxing Wei[1], Ruixiang Deng[1], Tianhang Xu[1], and Ying Xiang[2,*]

1 School of Mechatronic Engineering, Xi’an Technological University, Xi’an 710021, Shaanxi, China; qiaohu@xatu.edu.cn (Q.H.); RuiX_deng@163.com (D.-R.X.); 1922271857@qq.com (W.-Z.X.); xuworks@qq.com (X.-T.H.)

2 College of Mechanical and Electrical Engineering, Shaanxi University of Science and Technology, Xi’an 710021, Shaanxi, China; yingcara@hotmail.com

* Correspondence: yingcara@hotmail.com

Abstract： Multi-axis CNC abrasive belt grinding machine is an essential piece of equipment for processing the turbofan engine fan blades. The quality of blades determines whether engine performance can be further improved. As one of the important means to ensure the blade quality, the measurement of the blade is still in the stage of manually hand-held measurement, and it is urgent to introduce digital and intelligent means to improve this situation. In order to make the overall process of blade grinding and measurement digital and intelligent and make the CNC belt grinding machine integrated into the intelligent manufacturing system, its core is to upgrade the grinding machine by installing intelligent devices for the grinding machine. The primary premise of the upgrade is to reconstruct the post-processing system of the machine tool. Therefore, this article established a multi-axis CNC abrasive belt-grinding machine’s precise geometry assembly model, developed the post-process module based on the machine kinematics chain, established and validated a virtual grinding machine virtual simulation environment, and completed the experimental verification with a specific type of wide string hollow fan blade. The experimental results show the correctness and effectiveness of the post-processing module and the virtual simulation environment. The work of this paper provides an essential platform for the subsequent upgrade of the grinder and the installation of an in-machine measurement system.

Key words: CNC Abrasive Belt-Grinding Machine; Geometric Modeling; Postprocess; Virtual simulation; Hollow Blade

1. Introduction

The traditional machining methods of fan blades and large complex surfaces cannot guarantee accuracy and efficiency. The blades need to be manually polished after roughly ground by milling machines. [1-2] The introduction of NC abrasive belt grinding can be an excellent solution to the disadvantages of the

above situation because the abrasive belt grinding can grind the removal allowance and polish the profile. The NC belt-grinding machine produced by combining belt grinding with numerical control has the flexibility of belt grinding and the adaptability of CNC machine tools. Grinding with it will significantly improve the efficiency and surface quality of the complex surface machining[3-4]. In recent years, with the in-depth research on material removal allowance and grinding mechanism of belt grinding, belt grinding has become an important processing method for material removal manufacturing[5-6].

In blade mass production, grinding efficiency becomes particularly important. One of the best solutions is upgrading the off-machine detection to on-machine measurement[7]. In this way, the blade only needs one clamping during the process of "detection-grind-detection-regrinding", which can significantly improve the machining efficiency and quality of the blade. The existing belt grinding equipment has realized multi-axis CNC high-precision grinding. However, there are few CNC belt grinding machines equipped with an in-machine measuring module, so it is necessary to install an on-machine measuring module on the existing grinding machine for upgrading. The primary premise of machine tool upgrading and transformation is to reconstruct its post-processing system. Only after obtaining the open-source postprocessor can it provide an essential platform for the subsequent installation of on-machine measurement system. In order to integrate the CNC belt grinding machine into an intelligent manufacturing system, it is inevitable to establish the corresponding virtual simulation environment.

Converting tool position files into numerical control programs is usually called post-processing, and such transformation is necessary because the machine tool cannot recognize the tool position files. Tool contact coordinate and tool axis vector are the main parts of the tool position file, so the essence of post-processing is to convert the former into the motion of the machine tool straight axis and rotation axis[8]. Regarding the kinematics solution of five-axis machine tools, Qiu Zhoujingzi[9] proposed forward and inverse solution formulas for double-swing head machine tools and a general solution for miscutting caused by singular problems regarding the kinematics solution of five-axis machine tools. My Chu A et al. [10] established a new mathematical model which can obtain four important characteristics of machine tool kinematics and use them as

quantitative parameters to analyze and compare the kinematic performance of five-axis machine tools. He Yaoxiong et al. [11] proposed a general method for solving the kinematics of machine tools of arbitrary structure. Tang et al. [12] developed a five-axis machine tool postprocessor with angle optimization function by establishing a machine tool kinematics model. Zuo et al. [13] proposed a post-processing algorithm for five-axis positioning milling based on analyzing the structural characteristics of a five-axis milling machine. So and Jung[14] proposed a general method to derive the direct kinematics equation by considering the orthogonal joint of a five-axis machine and deduced a practical algorithm for the inverse kinematics equation of a five-axis machine. Boz and Lazoglu[15] introduced a processor for a table tilt five-axis machine tool based on generalized kinematics and variable feed rate. They proposed a method to eliminate motion singularity through spherical interpolation and NC data correction. Tutunea Fatan and Feng's study [16] focused on a general unified model for all five-axis machine tools with two rotating axes. They deduced the general coordinate transformation matrix of five-axis machine tools. Zhang[17] established a kinematic model of a double-tilted five-axis machine tool based on uniform coordinate transformation and kinematic chain relationship and developed a post-processing processor. For others, SøRby[18] proposed an algorithm to calculate the inverse kinematics of a nearly singular five-axis machine for path errors during five-axis milling. Sun et al. [19] established the kinematic model of the machine tool and developed the post-processing module of a new 3-coordinate linkage 5-axis machine tool by using inverse kinematics. Yang et al. [20-21] proposed a generalized kinematic model that allowed automatic configuration of all five-axis machine tools using screw theory. Zhou et al. [22] developed a postprocessor with optimized tool radius compensation for general machine tool configuration based on the generalized kinematic model. With the updating of machine tools and new functions, there have been postprocessors for more moving axes. For six-axis belt grinding machine tools, Luo et al. [23] proposed a kinematic analysis and optimization method for generating NC codes of grinding blades. Zhao Dan et al. [24] established a kinematic model of a new six-axis drilling machine through structural analysis and proposed an inverse kinematic strategy based on separation and combination. Tang et al. [25] developed a special post-processor for the turn-milling complex

machine tool with six linear axes and three rotating axes. Zhao et al. [26] studied the kinematic modeling and base calibration of a new automatic drilling and riveting system for aircraft panel assembly to improve its positioning accuracy. Yuen and Altintas[27] proposed a new NC code generation algorithm based on kinematics analysis of nine-axis micro-machine tools. Song et al. [28] proposed an effective post-processing algorithm for the nine-axis milling machine and a feed-rate optimization method for realizing double-tool synchronous milling. In terms of NC simulation, VERICUT, developed by CGTECH In the United States, is a software specially oriented to numerical control machining simulation. It has the function of analyzing simulation results and can be nested with other mainstream CAD/CAM software. VERICUT is a mature numerical control simulation software with many applications [29]. Some very mature CAD/CAM software abroad, such as Cimatron, MasterCAM, Pro/E, UG, etc., can also achieve the simulation processing function. The research on numerical control simulation technology in China is a little later than in developed countries and regions abroad. Nanjing University of Aeronautics and Astronautics also developed superman 2000CAD/CAM, which can realize the dynamic simulation of turning and milling [30]. Harbin Institute of Technology developed an NCMPS simulator, which can realize a 3D simulation of NC machining [31]. The SurfMill9.5 software developed by Beijing Fine Sculptural Group in 2021 integrates DT programming technology. By mapping actual production materials, process parameters and other information in the software, the virtual manufacturing platform, which is highly consistent with actual production, ensures that all production personnel can obtain accurate and consistent processing information in time. Based on this platform, this study will carry out a five-axis process analysis and optimization to eliminate the risk of five-axis processing in the software end, and facilitate a safe and smooth five-axis processing.

This article aims to upgrade an existing CNC abrasive belt grinding machine to provide open-source post-processing. Section 2 establishes the NC abrasive belt grinding machine geometry assembly model, and section 3 carries out the kinematics analysis of the machine tool. Section 4 verifies the effectiveness of the postprocessor by flat and hollow blade grinding and simulation experiment. At last, this paper ends with some conclusions.

2. Modeling and assembly of multi-axis CNC belt grinding machine

2.1 Structural analysis of CNC belt grinding machines

Figure 1 shows the MTS1600-500 CNC belt grinding machine. It has the characteristics of high precision, high speed, and high rigidity. It can realize copying grinding, constant pressure grinding, and NC grinding and can meet the finishing and polishing of the appearance of a wide-string hollow blade. Moreover, the blade shape precision is high, which ensures the blade's natural frequency and aerodynamic performance. However, the CNC belt grinding machine does not configure the in-machine measurement device. The grinding process of the whole process still needs several clamping so that the grinding accuracy and efficiency cannot be further improved.

Figue 1 The belt grinding machine

Installing the machine measuring device on the high-performance CNC machine tool is an effective way to improve the machine tool processing efficiency and the qualified rate of finished products without spending vast sums of money at the same time. As the basis for installing the measuring device on the machine, it is necessary to establish the grinder's accurate geometric assembly model first. In this paper, combining real machine analysis and drawing analysis is used to analyze the structure of machine tools before modeling. The multi-axis CNC abrasive belt-grinding machine has a complex structure, many parts, and a large appearance. However, its core motion framework comprises several components

or modules with different functions. By analyzing the structure of the multi-axis CNC belt grinder and excluding the parts that do not affect the virtual simulation, such as internal appliances, operation panel, and hydraulic system, as shown in Figure 2, the CNC belt grinder can be divided into seven basic modules: machine tool base, X-axis, Y-axis, Z-axis, B-axis, C-axis and tool components. The machine tool base includes: machine tool base body, longitudinal feed shaft, transverse feed shaft; X-axis includes: X-axis mobile components, worktable, pneumatic tailstock; C-axis includes: C-axis rotation components, sand-belt drive axle box, box shell; The tool assembly includes: tool shaft and the belt pulley; The Y-axis, Z-axis, and B-axis are all independent components.

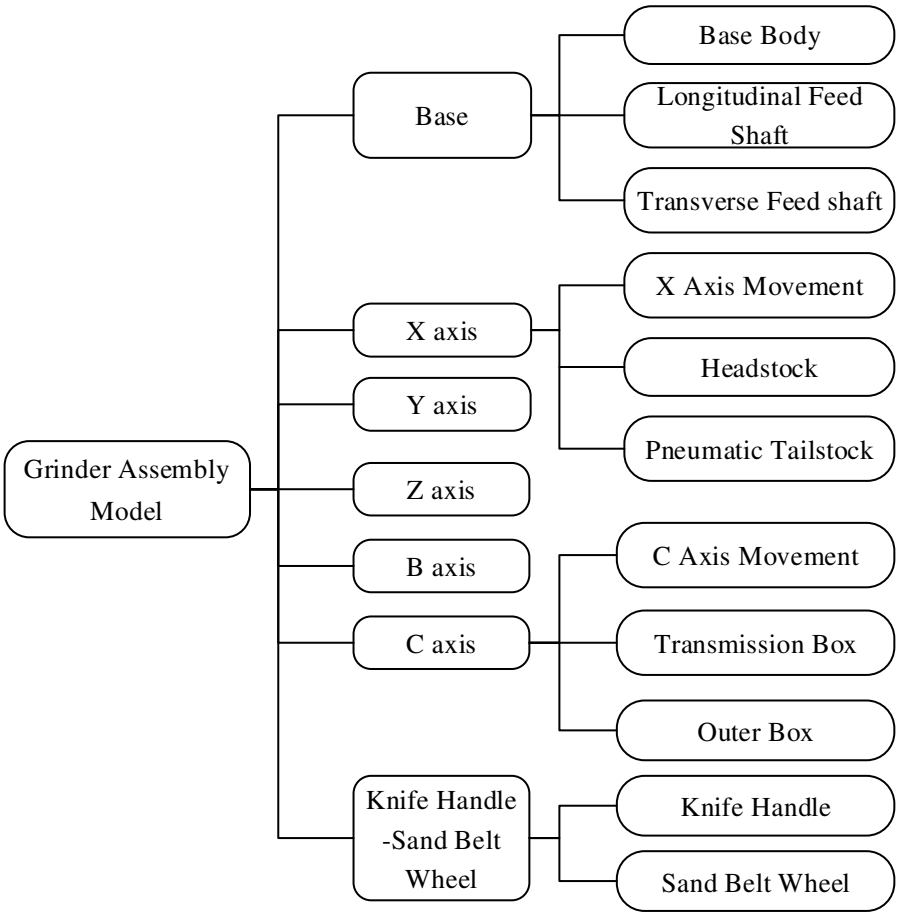

Figure 2 Explanation of the structure of the CNC belt grinding machine model

2.2 Obtaining assembly dimensions of grinding machine key shafts

The dimensions of the above components are obtained through the attached drawings and actual measurements of the machine tool, and the geometric model of the machine tool is established based on the data. It is also necessary to obtain

the assembly dimensions between the key axes of the machine tool to complete the assembly of each component. The process of obtaining this data is as follows. According to the structural analysis of the machine tool, the X-axis moving part installs on the longitudinal feed shaft of the machine tool base, and the A-axis moving part is installed on the X-axis table flange. The X-axis movement path is consistent with the direction of the extension line of the rotation center of the A axis, which determines the X direction of the machine tool coordinate system. The origin of the processing coordinate system locates at the center of the right end face of the fixture When the fixture fastens to the workbench, the center of the right end face of the fixture coincides with the center of the left end face of the workbench flange. As shown in Figure 3, the center of the left end face of the flange is O_{WT}. Then at X=0, that is, when the X-axis returns to zero, the origin of the machine tool coordinate system locates at the center of the left end face of the table flange in space.

Table 1 Travel table for each axis of the CNC belt grinding machine

Machine tool axes	Minimum stroke	Maximum stroke
X	-1876.7mm	-126.2mm
Y	-329mm	172mm
Z	183.7mm	685mm
A	-360°	360°
B	-45.2°	45.2°
C	-90.2°	90.2°

Table 1 shows the travel of each CNC abrasive belt grinder axis. It can be seen from the table that the Y-axis can return to zero, so move the Y-axis of the machine to Y=0, then move the X-axis to the maximum stroke, and finally move the Z-axis to the minimum stroke. Under the current position, mark the position that is 126.2mm from the center of the left end face of the flannel with X forward direction. The position of this point in space is the origin of the machine coordinate system O_M of the multi-axis CNC abrasive belt grinder, as shown in Figure 3.

At this point, mark 183.7mm from the positive direction of the Z-axis through the O_M point, and the marking point is determined as the center of the positioning hole on the left end face of the tool handle. When the machine moves to position X0Y0Z0A0B0C0, O_{WT} located in the center of the left end face of the flange on

the machine tool will coincide with this point. This point is the center of the positioning hole on the left end face of the tool handle in practice, and it is set as the machine tool reference point O_S, as shown in Figure 3. Figure 4 shows the specific location of the positioning hole center on the left end face of the tool holder.

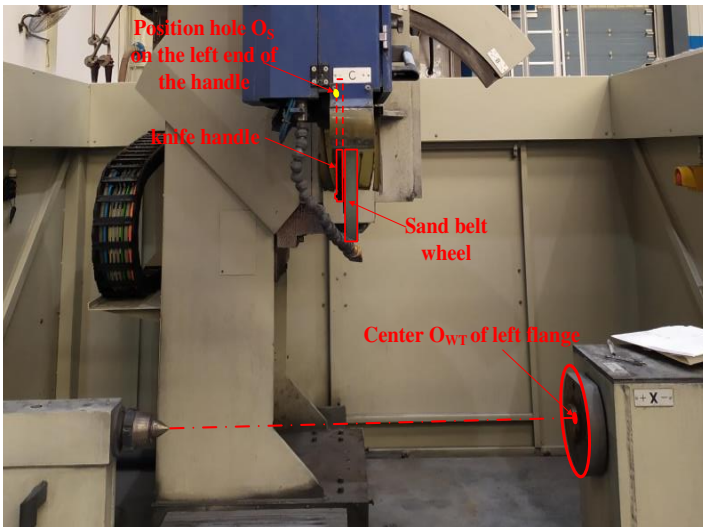

Figure 3 Process of obtaining machine reference points

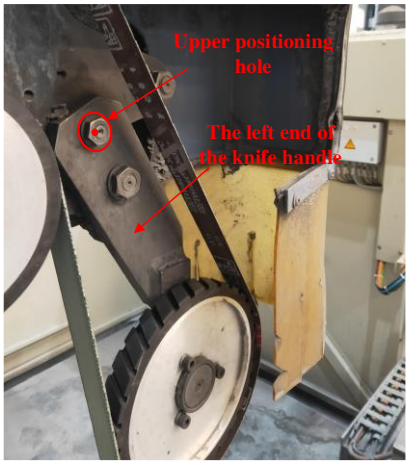

Figure 4 Position of the positioning hole on the left end face of the toolholder

Among them, the assembly between axis-B, axis-C and tool holder belt pulley directly affects the correctness of machine tool modeling. Exploring the relevant information of the machine tool to obtain a partly post-process program file, as shown in Figure 5. On the plane perpendicular to the B axis's rotational axis, there is a point with a horizontal distance of 42.672mm and a vertical distance of 270.649mm from the rotational axis of the B axis. On the plane perpendicular to the C axis of rotation, the horizontal distance between the same point and the C axis of rotation is 43.054mm, and the vertical distance is 78.051mm. It is determined that this point is the reference point in the machine tool O_S specified in the previous section.

```
42.672      #vek2distx=rbuf(1, 13 ) # X-Distance between 2nd axis and Mastercam-Origin3
0           #vek2disty=rbuf(1, 14 ) # Y-Distance between 2nd axis and Mastercam-Origin4
-270.649    #vek2distz=rbuf(1, 15 ) # Z-Distance between 2nd axis and Mastercam-Origin5
43.054              #vek3distx=rbuf(1, rc1)   # 60 X-Distance between 6th axis and Mastercam-Origin
78.051   #77.7      #vek3disty=rbuf(1, rc1)   # 61 Y-Distance between 6th axis and Mastercam-Origin
0                   #vek3distz=rbuf(1, rc1)   # 62 Z-Distance between 6th axis and Mastercam-Origin
```

Figure 5 Part of the post-processing file

The document and the machine coordinate system position determination use the machine reference point as the key position point. Determining the machine tool reference point is necessary for establishing an accurate geometric assembly model for this multi-axis CNC belt grinder. Based on the above data, the positions of B-axis coordinate system {B}, machine reference point coordinate system {S} and C-axis coordinate system {C} are established. B-axis coordinate system {B}locates on the B-axis rotation axis. C-axis coordinate system {C} is located on the C-axis rotation axis. Machine reference point coordinate system {S} locates at the center of the positioning hole on the left end face of the tool holder, and tool coordinate system {T} locates at the center of the bottom of the grinding belt wheel.

Figure 6(a) shows the position relationship between the coordinate system {B} and {S} in terms of the orientation of the front view. In terms of the coordinate system {B}, it is clear that $d_{BS,i} = -42.672mm;\ d_{BS,k} = 270.649mm$. Figure 2.6(b) shows the position relationship between the coordinate system {C} and {S} in terms of the direction of the top view. In terms of the coordinate system {C}, it is clear that $d_{CS,i} = -43.054mm;\ d_{CS,j} = -78.051mm$. The position relationship between the coordinate system {B} and {S} is the key dimensional data for subsequent assembly. And the distance between B-axis and C-axis is $d_{CS,i} = \left| d_{BS,i} - d_{CS,i} \right| = 0.382mm$, which shows that axes B and C do not intersect in space.

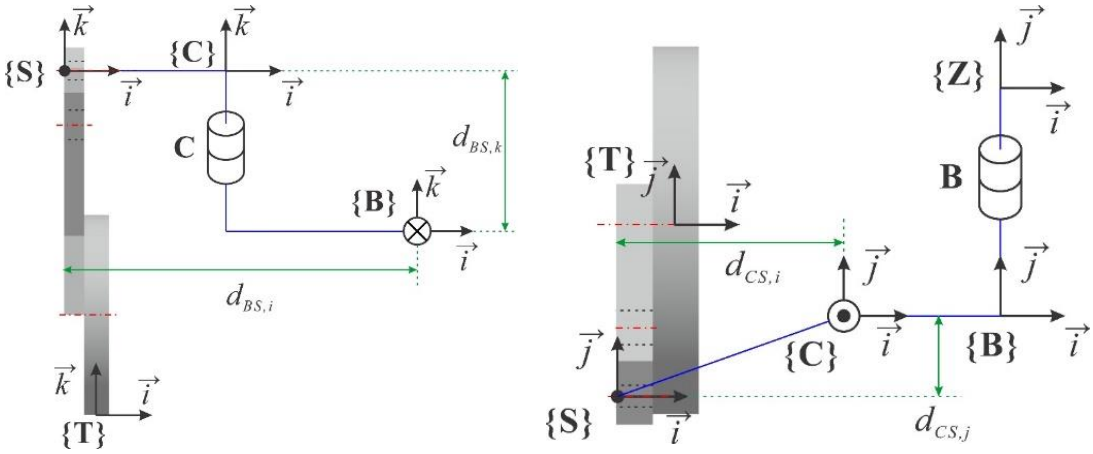

(a) Coordinate system {B} in relation to the position of {S}

(b) Coordinate system {C} in relation to the position of {S}

Figure 6 Location of the coordinate system coordinate system {S} in relation to the coordinate systems {B}, {C} and {T}

Let the machine reference point O_S (as well as the positioning hole center on the left end face of the tool holder) be the assembly origin, and use the assembly dimensions of the key axes above for assembly. Figure 7 shows the geometric model of the CNC belt grinder that has been assembled.

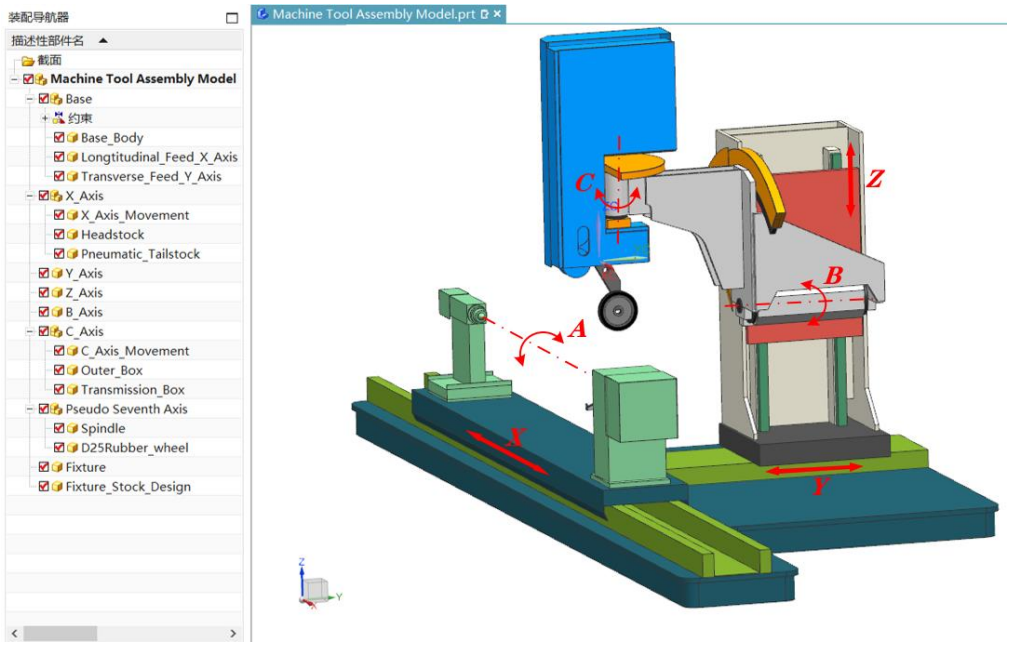

Figure 7 Overall assembly model of the MTS1600-500-6NC CNC belt grinding machine

3. Study of post-processing algorithm for multi-axis CNC belt grinder

3.1 Machine coordinate system and motion axis initial position definition

3.1.1 Definition of Coordinate System

For post-processing derivation of the multi-axis CNC belt grinder, it is essential to establish the coordinate system of each motion axis and the motion relationship between each axis first. In order to assist in deriving of the motion relationships, the next step needs to establish a reference coordinate system {MF} (machine base coordinate system), as shown in Figure 8(a). {MF} is a fixed spatial coordinate system, as shown in Figure 8(b). Within the coordinate system{MF}, let $\vec{i}_{MF}$ define the direction along with the X-axis guide of the machine tool, positive to the right. Let $\vec{j}_{MF}$ define the direction along with the Y-axis guide of

the CNC grinding machine, positive away from the X-axis guide. Let $\vec{k}_{MF}$ define the direction along with the Z-axis of the CNC grinding machine, positive upward, and the coordinate origin is the intersection of the A-axis and the B-axis common vertical line of the CNC grinding machine on the A-axis. The coordinate system {WT} is the table coordinate system, as shown in Figure 8(b), and the origin of this coordinate system locates at the intersection of the left end face of the flange and its rotation center (A-axis).

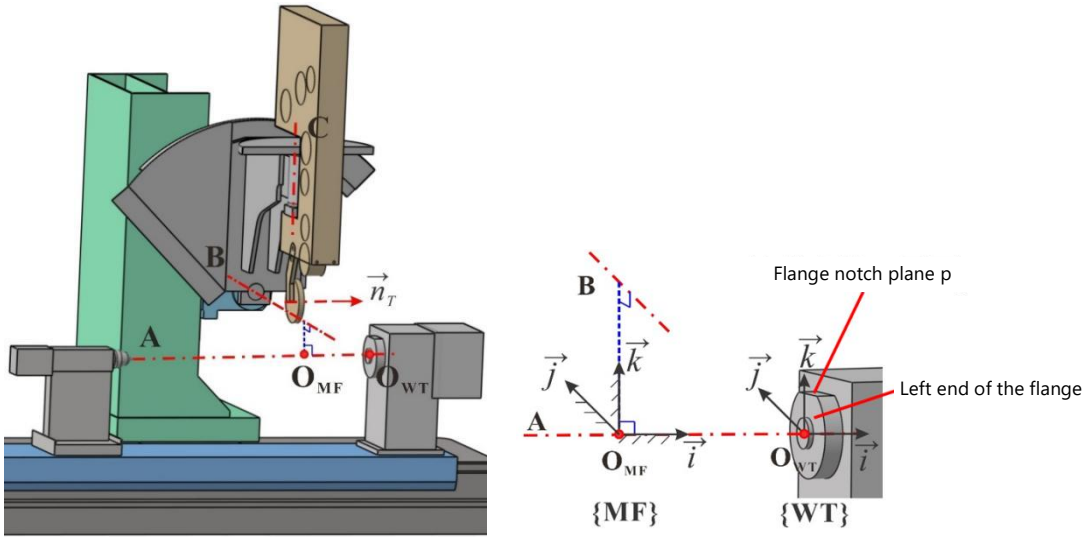

(a) Definition of the position of the reference coordinate system and the table coordinate system

(b) Definition of reference coordinate system and table coordinate system direction

Figure 8 Schematic diagram of the reference and table co-ordinate systems

3.1.2 Definition of the initial position of the machine motion axis

After defining the position of the reference coordinate system {MF}, it is also necessary to define the initial position of the multi-axis CNC belt grinder in this coordinate system (the position where the motion of the CNC grinder is zero). First, define the initial position of each rotary axis, as shown in Figure 8(b) above, with the initial position of the A-axis set to be parallel to the flange notch plane *p* and plane $\vec{i}_{MF}$-$\vec{j}_{MF}$. The initial position of the B-axis is set to have the C-axis parallel to $\vec{k}_{MF}$; the initial position of the C-axis is to have the central axis of the grinding wheel $\vec{n}_T$ parallel to $\vec{i}_{MF}$. Figure 9(a) shows the initial position of the linear axis of the multi-axis CNC belt grinder, and the initial position of the X-

axis is defined as O_{MF} , coinciding with O_{WT} . As shown in Figure 9(c), the initial position of the Y-axis is defined as the C-axis in plane $\vec{i}_{MF}$-$\vec{k}_{MF}$.

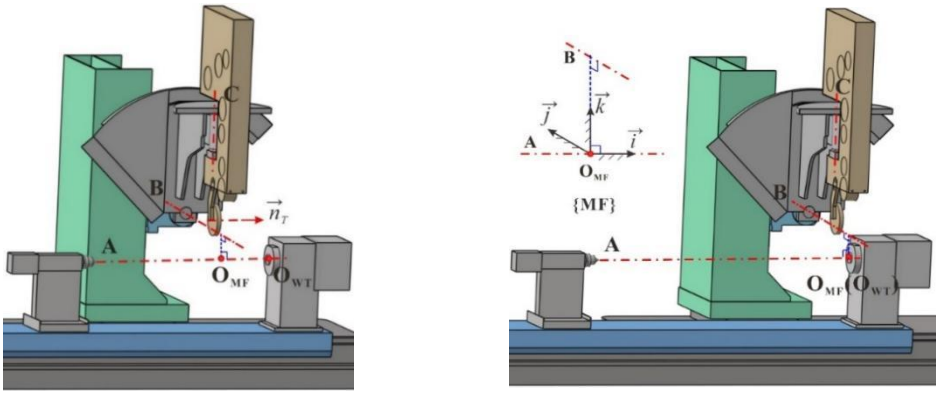

(a) Schematic diagram of the initial X-axis position

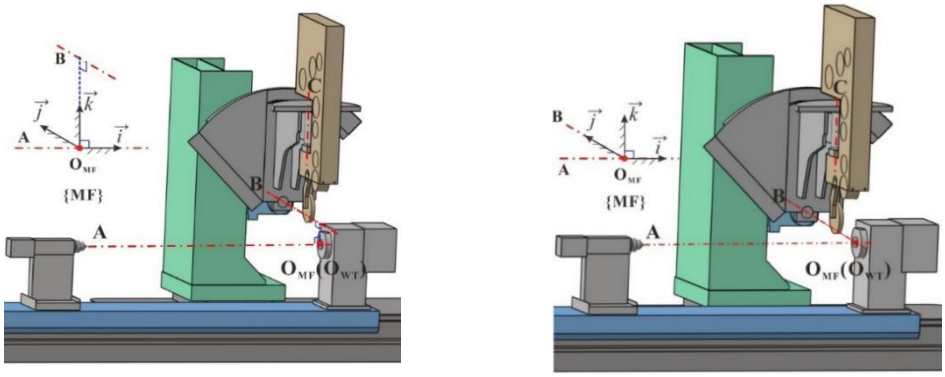

(b) Schematic diagram of the initial Z-axis position

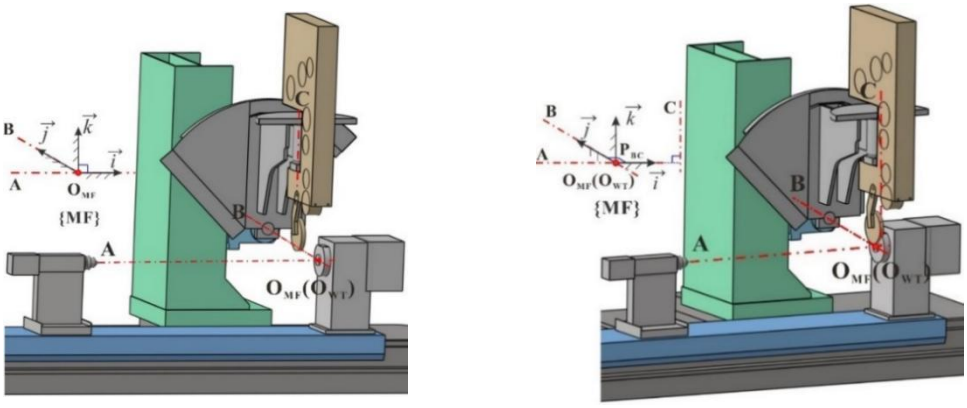

(c) Schematic diagram of the initial Y-axis position

Figure 9 Definition of the initial position of the linear axes in the {MF} coordinate system

3.2 Building machine tool kinematic chains

3.2.1 Machine table group kinematic chain

The derivation starts with the machine table group (workpiece motion chain). As shown in Figure 10 below, the motion first moves X from the X-axis coordinate system along the $\vec{i}$ -direction of {MF} and then passes to the A-axis coordinate system. That is, the X-axis coordinate system moves X distance relative to the {MF} coordinate system.

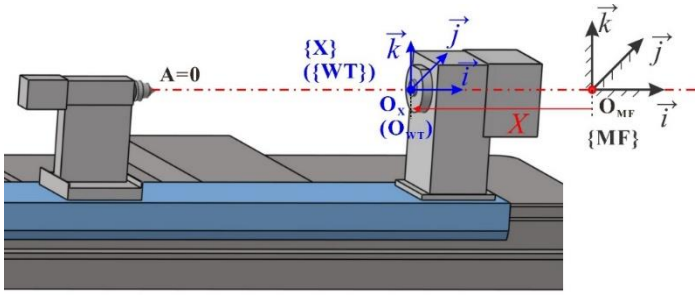

Figure 10 Schematic diagram of motion transfer between X coordinate system and {MF} coordinate system

From the schematic diagram of the motion transfer between the X coordinate system and the {MF} coordinate system, the transformation matrix ${}^{MF}T_X$ expressed in the machine base coordinate system {MF} (reference coordinate system) for the points in the X coordinate system can be obtained.

$$ {}^{MF}T_X = \begin{bmatrix} 1 & 0 & 0 & X \\ 0 & 1 & 0 & 0 \\ 0 & 0 & 1 & 0 \\ 0 & 0 & 0 & 1 \end{bmatrix} \tag{3.1} $$

As shown in Figure 11, the A-axis coordinate system rotates by an angle A around the $\vec{i}$ -direction of the X-axis coordinate system to transfer the motion to the workpiece. That is, the {WT} coordinate system rotates by an angle A for the X-axis coordinate system.

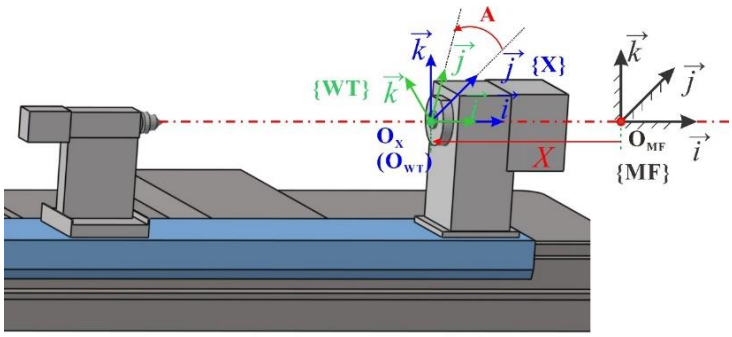

Figure 11 Schematic diagram of motion transfer between {WT} coordinate system and X coordinate system

From the schematic diagram of motion transfer between the {WT} coordinate system and the X coordinate system, the transformation matrix ${}^{X}T_{WT}$ expressed in the X coordinate system for the points in the table coordinate system {WT} is obtained as:

$$ {}^{X}T_{WT} = \begin{bmatrix} 1 & 0 & 0 & 0 \\ 0 & \cos A & -\sin A & 0 \\ 0 & \sin A & \cos A & 0 \\ 0 & 0 & 0 & 1 \end{bmatrix} \tag{3.2} $$

The kinematic chain of the multi-axis CNC belt grinder table group can be obtained by combining the motion transfer of the X coordinate system with the {MF} coordinate system and the {WT} coordinate system, as shown in Figure 12.

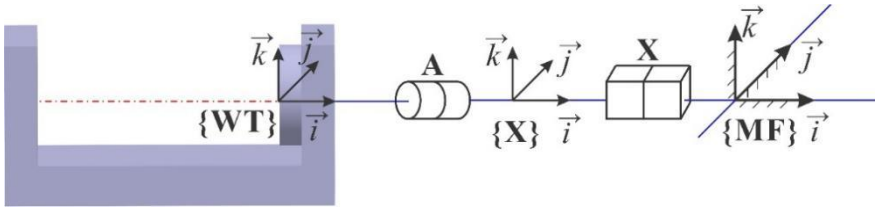

Figure 12 Schematic diagram of WT-X-MF kinematic chain

3.2.2 Machine tool cluster kinematics chain

(1) MF-Y-Z kinematic chain

The kinematic chain of the machine tool group is analyzed, and the motion is transferred from the {MF} coordinate system to the Y-axis coordinate system and then to the Z-axis coordinate system. Since both Y-axis and Z-axis are linear axes, the kinematic relationship is relatively simple. As shown in Figure 13, the motion is first moved Y by the Y-axis coordinate system along the $\vec{j}$ -direction of {MF} and then passed to the Z-axis coordinate system. That is, the Y-axis coordinate system moves Y distance relative to the {MF} coordinate system, and the Z-axis coordinate system moves Z distance relative to the Y coordinate system.

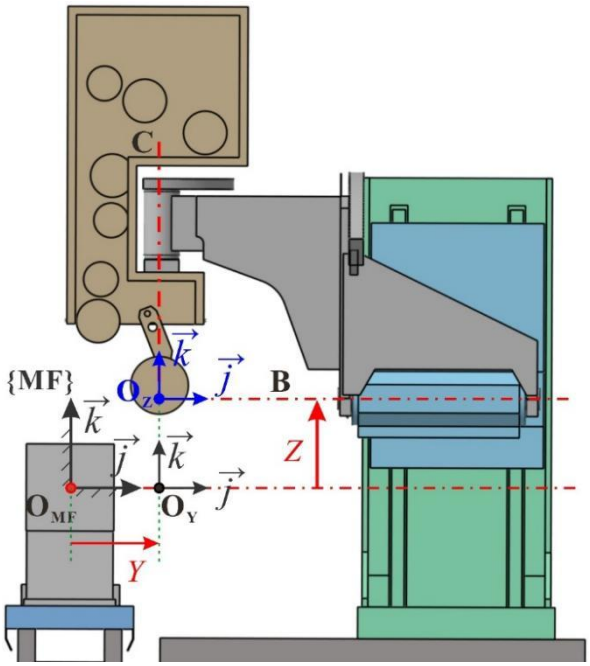

Figure 13 Schematic diagram of motion transfer between {MF} coordinate system and Y and Z coordinate system

The transformation matrix ${}^{MF}T_Y$ expresses the points of the {Y} coordinate system in the machine base coordinate system {MF} (reference coordinate system) obtained from the motion transfer of the {MF} coordinate system and the Y coordinate system as:

$$ {}^{MF}T_Y = \begin{bmatrix} 1 & 0 & 0 & 0 \\ 0 & 1 & 0 & Y \\ 0 & 0 & 1 & 0 \\ 0 & 0 & 0 & 1 \end{bmatrix} \tag{3.3} $$

The transformation matrix ${}^{Y}T_Z$ expresses the points of the {Y} coordinate system for in the {Z} coordinate system obtained from the motion transfer of the Y coordinate system and the Z coordinate system.

$$ {}^{Y}T_Z = \begin{bmatrix} 1 & 0 & 0 & 0 \\ 0 & 1 & 0 & 0 \\ 0 & 0 & 1 & Z \\ 0 & 0 & 0 & 1 \end{bmatrix} \tag{3.4} $$

The multi-axis CNC belt grinder MF-Y-Z kinematic chain can be obtained from the {MF} coordinate system and the Y and Z coordinate system motion transfer, as shown in Figure 14.

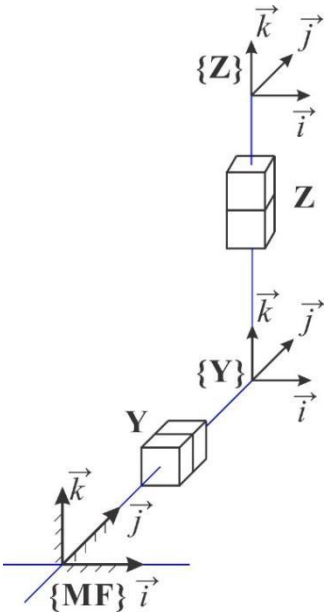

Figure 14 Schematic diagram of MF-Y-Z kinematic chain

(2) MF-Y-Z-B-C kinematic chain

As shown in Figure 15, the B-axis of the abrasive belt grinder is mounted on the Z-axis. The B-axis is the axis of rotation. The B-axis coordinate system will make a rotational motion relative to the Z-axis coordinate system. The B-axis coordinate system rotates by an angle B in the $\vec{j}$ -direction around the Z-axis coordinate system.

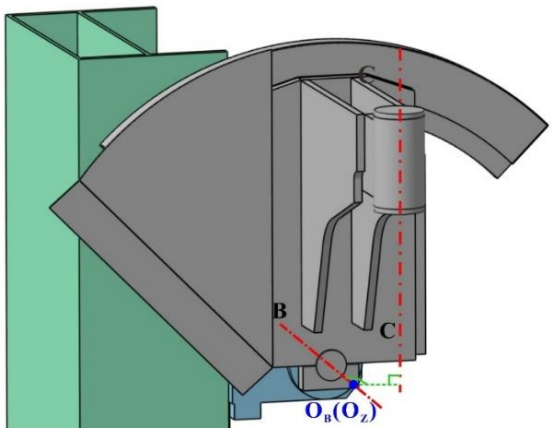

Figure 15 Schematic diagram of motion transfer between Z coordinate system and B coordinate system

The transformation matrix ${}^{Z}T_{B}$ expresses the points of the {B} coordinate system in the {Z} coordinate system obtained from the motion transfer of the Z coordinate system and the B coordinate system:

$$ {}^{Z}T_{B} = \begin{bmatrix} \cos B & 0 & \sin B & 0 \\ 0 & 1 & 0 & 0 \\ -\sin B & 0 & \cos B & 0 \\ 0 & 0 & 0 & 1 \end{bmatrix} \tag{3.5} $$

The previous structural analysis of the machine determines that the B-axis and C-axis of this multi-axis CNC belt grinder do not intersect in space, as shown in Figure 16 below, and the common vertical distance between the two axis axes is $d_{BC,i}$.

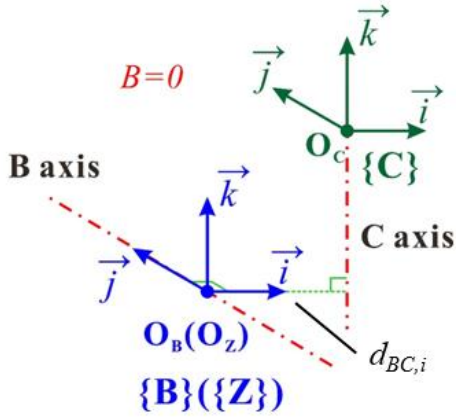

Figure 16 Schematic diagram of B and C axis position deviation

Therefore, there is first a translation matrix T between the B-axis coordinate system and the C-axis coordinate system:

$$ T = \begin{bmatrix} 1 & 0 & 0 & d_{BC,i} \\ 0 & 1 & 0 & 0 \\ 0 & 0 & 1 & 0 \\ 0 & 0 & 0 & 1 \end{bmatrix} \tag{3.6} $$

Furthermore, axis C is a rotary axis mounted on the B axis, which can make the rotary motion, as shown in Figure 17.

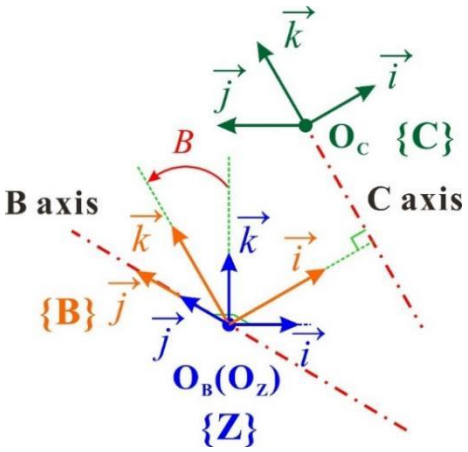

Figure 17 Schematic diagram of motion transfer between {B} coordinate system and {C} coordinate system

Then, the transformation matrix ${}^{B}T_{C}$ expresses the points of the {C} coordinate system in the {B} coordinate system obtained from the motion transfer of the{B} coordinate system and the {C} coordinate system:

$$ {}^{B}T_{C} = \begin{bmatrix} 1 & 0 & 0 & d_{BC,i} \\ 0 & 1 & 0 & 0 \\ 0 & 0 & 1 & 0 \\ 0 & 0 & 0 & 1 \end{bmatrix} \begin{bmatrix} \cos C & -\sin C & 0 & 0 \\ \sin C & \cos C & 0 & 0 \\ 0 & 0 & 1 & 0 \\ 0 & 0 & 0 & 1 \end{bmatrix} \tag{3.7} $$

Figure 18 shows a multi-axis CNC belt grinder MF-Y-Z-B-C kinematic chain obtained.

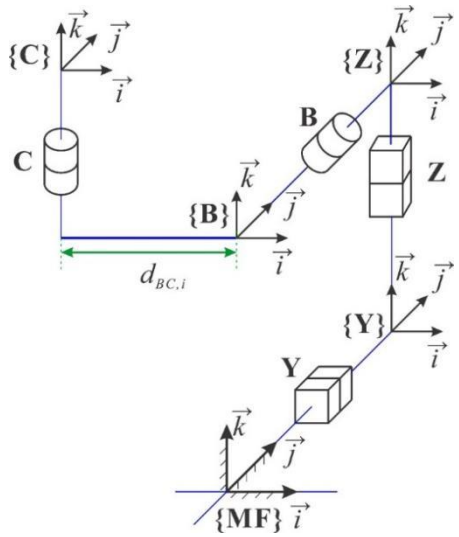

Figure 18 MF-Y-Z-B-C kinematic chain

(3) MF-Y-Z-B-C-S-T kinematic chain

The above analysis derives the coordinate transformation matrix from the MF coordinate system to the C-axis coordinate system. The transformation matrix from the C-axis coordinate system to the reference point coordinate system of the abrasive belt grinder and then to the tool coordinate system still needs to be analyzed. The analysis of the key data during the overall assembly of the CNC belt grinder in the previous chapter obtains the relationship between the reference point coordinate system {S} and the coordinate systems {B}, {C}, and {T}, as shown in the previous Figure 18. The transformation matrix ${}^{C}T_{S}$ of the points in the {S} coordinate system expressed in the {C} coordinate system is obtained from the positions relationship between the coordinate system {C} and {S}.

$$ {}^{C}T_{S} = \begin{bmatrix} 1 & 0 & 0 & d_{CS,i} \\ 0 & 1 & 0 & d_{CS,j} \\ 0 & 0 & 1 & 0 \\ 0 & 0 & 0 & 1 \end{bmatrix} \tag{3.8} $$

According to the analysis of the machine structure and Figure 18, let the center of the positioning hole on the left end face of the tool holder be the origin of the coordinate system {S}, and the center of the lower contact surface of the abrasive belt wheel be the origin of the coordinate system {T}. Figure 19 shows the established relationship between the position of the coordinate system {S} and {T}. The calculate results are: $d_{ST,i}$=43mm； $d_{ST,j}$=79.2mm； $d_{ST,k}$=350mm.

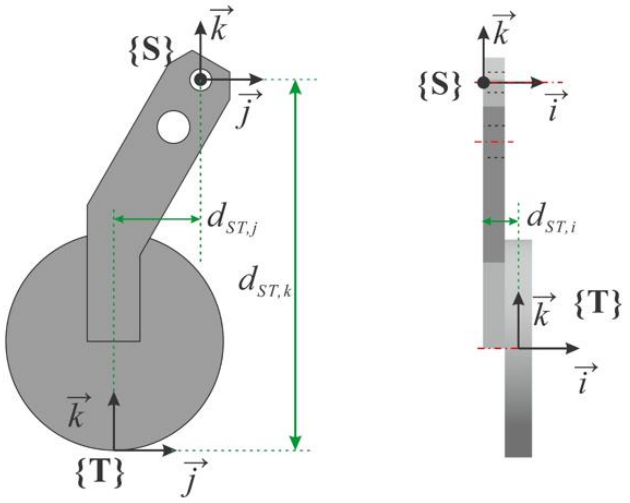

Figure 19 The position relationship between coordination {S}and{T}

The transformation matrix ${}^{S}T_{T}$ of the points in the tool coordinate system {T} expressed in the {S} coordinate system can be obtained from the above figure：

$$ {}^{S}T_{T} = \begin{bmatrix} 1 & 0 & 0 & d_{ST,i} \\ 0 & 1 & 0 & d_{ST,j} \\ 0 & 0 & 1 & d_{ST,k} \\ 0 & 0 & 0 & 1 \end{bmatrix} \tag{3.9} $$

A multi-axis CNC belt grinding machine MF-Y-Z-B-C-S-T kinematic chain can be obtained, as shown in Figure 20.

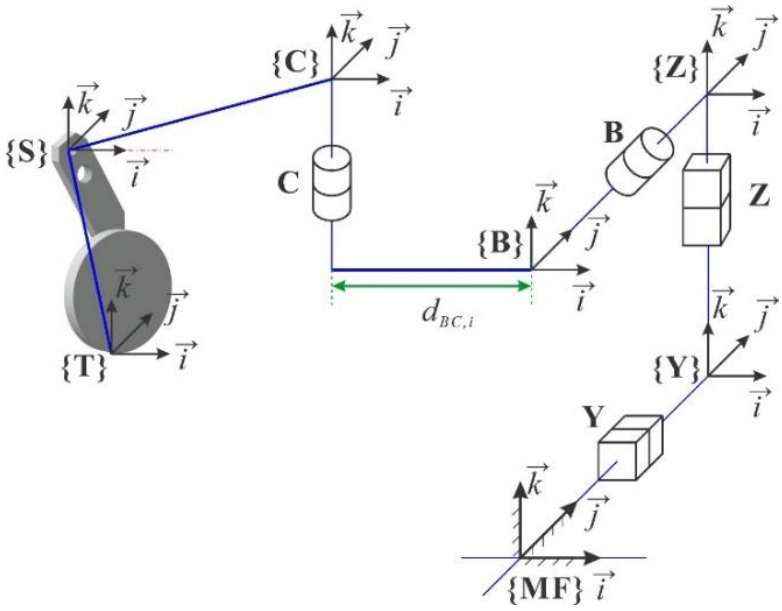

Figure 20 The position relationship between coordination {S}and{T}

3.2.3 The kinematic chain of the whole machine tool

The overall kinematic chain of the machine consists of the table group kinematic chain and the tool group kinematic chain. That is, {WT}-X-{MF}-Y-Z-B-C-S-T, and the overall kinematic chain of the multi-axis CNC belt grinder is obtained as shown in Figure 21.

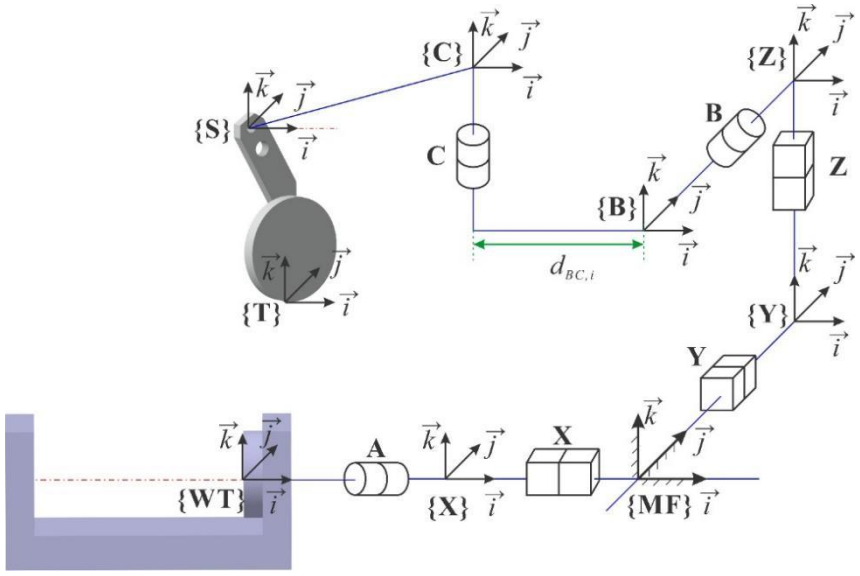

Figure 21 CNC belt grinding machine kinematic chain

3.3 Post-processing process derivation

3.3.1 Deriving the coordinate transformation matrix

According to the analysis of the kinematic chain of the machine table group, the transformation matrix ${}^{MF}T_{WT}$ of the points in the table coordinate system {WT} expressed in the machine base coordinate system {MF} (reference coordinate system) can be obtained by combining equations (3.1) and (3.2).

$$ {}^{MF}T_{WT} = {}^{MF}T_{X}\,{}^{X}T_{WT} = \begin{bmatrix} 1 & 0 & 0 & X \\ 0 & 1 & 0 & 0 \\ 0 & 0 & 1 & 0 \\ 0 & 0 & 0 & 1 \end{bmatrix} \begin{bmatrix} 1 & 0 & 0 & 0 \\ 0 & \cos A & -\sin A & 0 \\ 0 & \sin A & \cos A & 0 \\ 0 & 0 & 0 & 1 \end{bmatrix} = \begin{bmatrix} 1 & 0 & 0 & X \\ 0 & \cos A & -\sin A & 0 \\ 0 & \sin A & \cos A & 0 \\ 0 & 0 & 0 & 1 \end{bmatrix} \tag{3.10} $$

According to the analysis of the kinematic chain of the machine tool group, the transformation matrix ${}^{MF}T_{T}$ of the points in the tool coordinate system {T} expressed in the machine base coordinate system {MF} (reference coordinate system) can be obtained by combining equations (3.3) to (3.9).

$$ \begin{aligned} {}^{MF}T_{T} &= {}^{MF}T_{Y}\,{}^{Y}T_{Z}\,{}^{Z}T_{B}\,{}^{B}T_{C}\,{}^{C}T_{S}\,{}^{S}T_{T} \\ &= \begin{bmatrix} 1 & 0 & 0 & 0 \\ 0 & 1 & 0 & Y \\ 0 & 0 & 1 & 0 \\ 0 & 0 & 0 & 1 \end{bmatrix} \begin{bmatrix} 1 & 0 & 0 & 0 \\ 0 & 1 & 0 & 0 \\ 0 & 0 & 1 & Z \\ 0 & 0 & 0 & 1 \end{bmatrix} \begin{bmatrix} \cos B & 0 & \sin B & 0 \\ 0 & 1 & 0 & 0 \\ -\sin B & 0 & \cos B & 0 \\ 0 & 0 & 0 & 1 \end{bmatrix} \begin{bmatrix} 1 & 0 & 0 & d_{BC,i} \\ 0 & 1 & 0 & 0 \\ 0 & 0 & 1 & 0 \\ 0 & 0 & 0 & 1 \end{bmatrix} \\ &\quad \begin{bmatrix} \cos C & -\sin C & 0 & 0 \\ \sin C & \cos C & 0 & 0 \\ 0 & 0 & 1 & 0 \\ 0 & 0 & 0 & 1 \end{bmatrix} \begin{bmatrix} 1 & 0 & 0 & d_{CS,i} \\ 0 & 1 & 0 & d_{CS,j} \\ 0 & 0 & 1 & 0 \\ 0 & 0 & 0 & 1 \end{bmatrix} \begin{bmatrix} 1 & 0 & 0 & d_{ST,i} \\ 0 & 1 & 0 & d_{ST,j} \\ 0 & 0 & 1 & d_{ST,k} \\ 0 & 0 & 0 & 1 \end{bmatrix} \end{aligned} \tag{3.11} $$

After sorting, we can obtain ${}^{MF}T_{T}$:

$$ {}^{MF}T_{T} = {}^{MF}T_{Y}\,{}^{Y}T_{Z}\,{}^{Z}T_{B}\,{}^{B}T_{C}\,{}^{C}T_{S}\,{}^{S}T_{T} = \begin{bmatrix} \cos B\cos C & -\cos B\sin C & \sin B & p \\ \sin C & \cos C & 0 & m \\ -\cos C\sin B & \sin B\sin C & \cos B & n \\ 0 & 0 & 0 & 1 \end{bmatrix} \tag{3.12} $$

Where the values of p,m,n are:

$$ p = (d_{BS,k} + d_{ST,k})\sin B + (d_{BS,i} - d_{CS,i})\cos B + (d_{CS,i} + d_{ST,i})\cos B\cos C - (d_{CS,j} + d_{ST,j})\cos B\sin C $$

$$ m = Y + (d_{CS,i} + d_{ST,i})\sin C + (d_{CS,j} + d_{ST,j})\cos C $$

$$ n = Z + (d_{BS,k} + d_{ST,k})\cos B - (d_{BS,i} - d_{CS,i})\sin B - (d_{CS,i} + d_{ST,i})\cos C\sin B + (d_{CS,j} + d_{ST,j})\sin B\sin C $$

From equations (3.10) and (3.12), the transformation matrix ${}^{WT}T_T$ of the points in the tool coordinate system {T} expressed in the table coordinate system {WT} is obtained:

$$ {}^{WT}T_T = {}^{WT}T_{MF}\,{}^{MF}T_T = ({}^{MF}T_{WT})^{-1}\,{}^{MF}T_T = \begin{bmatrix} 1 & 0 & 0 & X \\ 0 & \cos A & -\sin A & 0 \\ 0 & \sin A & \cos A & 0 \\ 0 & 0 & 0 & 1 \end{bmatrix} \cdot {}^{MF}T_T = $$

$$ \begin{bmatrix} \cos B\cos C & -\cos B\sin C & \sin B & -X+p \\ \cos A\sin C-\sin A\sin B\sin C & \cos A\cos C-\sin A\sin B\sin C & \sin A\cos B & \cos A\cdot m+\sin A\cdot n \\ -\sin A\sin C-\cos A\cos C\cos B & \cos A\sin B\sin C & \cos A\cos B & \cos A\cdot n-\sin A\cdot m \\ 0 & 0 & 0 & 1 \end{bmatrix} \quad (3.13) $$

A coordinate system is determined by the position of the origin and the direction of the three axes. So, the first column of the transformation matrix ${}^{WT}T_T$ of the points in the tool coordinate system {T} expressed in the table coordinate system {WT} represents the X direction of the tool coordinate system {T} under the {WT} coordinate system, the second column represents the Y direction, the third column represents the Z direction, and the fourth column represents the position of the origin.

Let the knife contact be $p_c = (p_{c,x}, p_{c,y}, p_{c,z})$, the tool axis vector be $p_n = (p_{n,x}, p_{n,y}, p_{n,z})$. The table coordinate system {WT} of this multi-axis CNC belt grinder coincides with the programmed coordinate system, and the origin of the tool coordinate system {T} is expressed under the programmed coordinate system as follows.

$$ \begin{bmatrix} p_{c,x} \\ p_{c,y} \\ p_{c,z} \\ 1 \end{bmatrix} = {}^{WT}T_T \begin{bmatrix} 0 \\ 0 \\ 0 \\ 1 \end{bmatrix} = \begin{bmatrix} -X+p \\ \cos A\cdot m+\sin A\cdot n \\ \cos A\cdot n-\sin A\cdot m \\ 1 \end{bmatrix} \quad (3.14) $$

The expression of the unit vector in the Z direction in the tool coordinate system {T} under {WT} is the expression of the unit normal vector of the contact point on the surface in the coordinate system {WT}:

$$ \begin{bmatrix} p_{n,x} \\ p_{n,y} \\ p_{n,z} \\ 1 \end{bmatrix} = {}^{WT}T_T \begin{bmatrix} 0 \\ 0 \\ 1 \\ 0 \end{bmatrix} = \begin{bmatrix} \sin B \\ \sin A\cos B \\ \cos A\cos B \\ 0 \end{bmatrix} \quad (3.15) $$

3.3.2 Determining the machine home position offset

In section 2.3 has been determined that when X = 0, the machine tool coordinate system origin is located in the center of the circle on the left end face of the table flange. When the machine tool moves to the X0Y0Z0A0B0C0 position, the machine tool is located in the center of the left end face of the flange point set as a reference point. This reference point in practice for the center of the positioning hole on the left end face of the tool holder. The displacement (or rotation) of each machine tool axis under the machine tool coordinate system is zero. The initial position of the A-axis, B-axis, and C-axis is the same as in the machine tool base coordinate system. The definition of the initial position of the linear axis of a multi-axis CNC belt grinding machine differs from that under the machine base coordinate system. Figure 22(a) shows the current assembly position of the CNC belt grinder. The Y-axis is clear to zero when the vertical line over the machine reference point O_S intersects with the line where $\mathbf{i}_{WT}$ is located, as shown in Figure 22(b). The X-axis is clear to zero when the vertical line over the point O_S intersects with the point O_{WT} at Y=0, as shown in Figure 22(c). The Z-axis is clear to zero when the point O_S coincides with the O_{WT} at X=0 and Y=0, as shown in Figure 22(d). When the machine tool axis moves to this position, the machine tool coordinate system origin is located at the center of the table flange left-end face circle in space. Figure 22 also shows why the X-axis and Z-axis cannot return to zero because this position will produce serious interference.

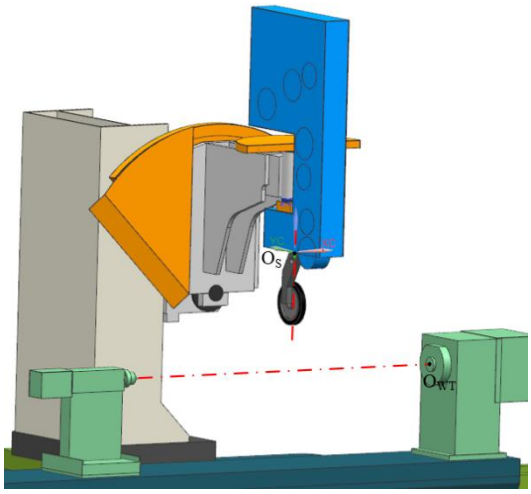

(a) Current assembly position of the CNC belt grinding machine

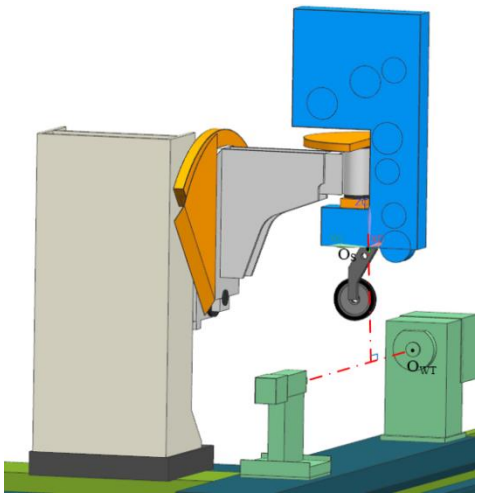

(b) Initial position of the Y-axis in the machine coordinate system

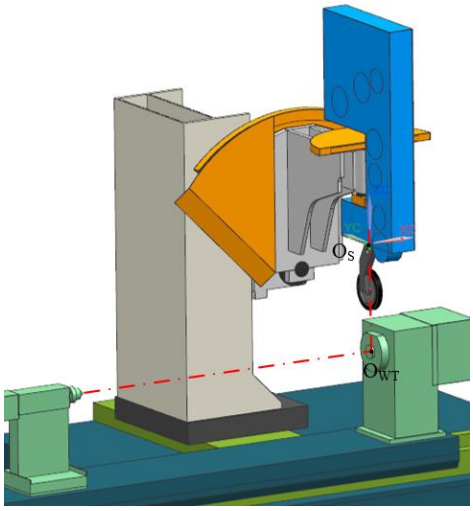

(c) Initial position of the X and Y axes in the machine coordinate system

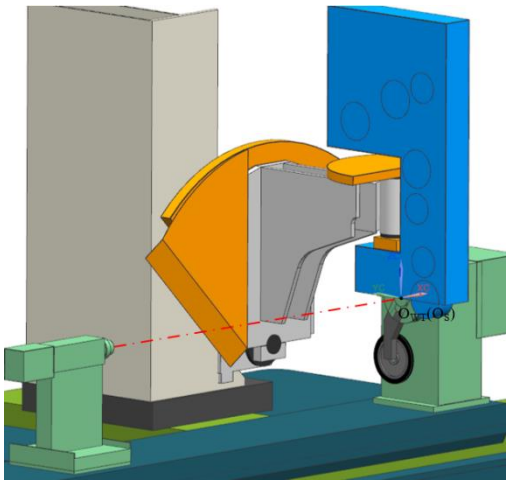

(d) Initial positions of the X, Y and Z axes in the machine's coordinate system

Figure 22 Initial position of each axis in the machine coordinate system

A comparison shows that the initial positions under the machine tool coordinate system {M} are offset from the initial positions under the reference coordinate system {MF} established in the derivation of the kinematic chain, as shown in Table 2:

Table 2 Table defining the difference between the two coordinate systems back to zero

Motion axis zeroing	Coordinate system	Definition method	Offset
X-axis zeroing	{MF}	The point of intersection of the A-axis and B-axis common plumb line coincides with O_{WT}	$d_{BS,i}$
	{M}	The intersection of the A-axis and the {S}-point plumb line coincides with O_{WT}	
Y-axis zeroing	{MF}	C-axis axis over O_{WT}	$d_{CS,j}$
	{M}	{S} point plumb line through O_{WT}	
Z-axis zeroing	{MF}	B-axis axis over O_{WT}	$d_{BS,k}$
	{M}	{S} point plumb line through O_{WT}	

As can be seen from Table 2, the reference coordinate system {MF} established by considering the kinematic chain derivation is offset from the machine tool coordinate system set up by the machine tool manufacturer, with:

$$\begin{cases} X_M = -X + d_{BS,i} \\ Y_M = Y + d_{CS,j} \\ Z_M = Z + d_{BS,k} \\ A_M = -A + 360^{\circ} \\ B_M = B \\ C_M = C \end{cases} \tag{3.16}$$

Where the subscripts with M are the values of the axes of motion in the machine's coordinate system.

From the above equation, it follows that:

$$\begin{cases} X = -X_M + d_{BS,i} \\ Y = Y_M - d_{CS,j} \\ Z = Z_M - d_{BS,k} \\ A = -A_M + 360^{\circ} \\ B = B_M \\ C = C_M = 0 \end{cases} \tag{3.17}$$

3.3.3 Solving the coordinate transformation matrix

Substituting the bias-transformed machine coordinate values into the tool axis vector obtained from equation (3.15) gives:

$$\begin{cases} p_{n,x} = \sin B_M \\ p_{n,y} = -\sin A_M \cos B_M \quad B_M \in \left[-45.2^{\circ}, 45.2^{\circ}\right], \cos B_M > 0 \\ p_{n,z} = \cos A_M \cos B_M \end{cases} \tag{3.18}$$

From the above equation, it follows that: $B_M = \arcsin(p_{n,x})$,and the following:

$$\begin{aligned} &\cos B_M = \sqrt{1-(p_{n,x})^2} \\ &\sin A_M = -p_{n,y} / \cos B_M = -p_{n,y} / \sqrt{1-(p_{n,x})^2} \\ &\cos A_M = p_{n,z} / \cos B_M = p_{n,z} / \sqrt{1-(p_{n,x})^2} \end{aligned} \tag{3.19}$$

In particular,

$$\text{if } p_{n,y} < 0\text{:}\quad A_M = \arccos(p_{n,z} / \cos B_M) = \arccos(p_{n,z} / \sqrt{1-(p_{n,x})^2})$$

$$\text{if } p_{n,y} > 0\text{:}\quad A_M = 2\pi - \arccos(p_{n,z} / \cos B_M) = 2\pi - \arccos(p_{n,z} / \sqrt{1-(p_{n,x})^2})$$

$$\text{if } p_{n,y} = 0 \text{且} p_{n,z} > 0\text{:}\quad A_M = 0$$

$$\text{if } p_{n,y} = 0 \text{且} p_{n,z} < 0\text{:}\quad A_M = \pi$$

$$\text{if } p_{n,y} = 0 \text{且} p_{n,z} = 0\text{:}\quad A_M = \pi / 2$$

Once the expression for the axis of rotation is obtained, this gives:

$$\begin{cases} X_M = p_{c,x} - d_{BS,i}(\cos B_M - 1) - d_{BS,k} \sin B_M - d_{ST,k} \sin B_M - d_{ST,i} \cos B_M \\ Y_M = p_{c,y} \cos A_M + p_{c,z} \sin A_M - d_{ST,j} \\ Z_M = -p_{c,y} \sin A_M + p_{c,z} \cos A_M - d_{BS,k}(\cos B_M - 1) + d_{BS,i} \sin B_M - d_{ST,k} \cos B_M + d_{ST,i} \sin B_M \end{cases} \tag{3.20}$$

A post-processing algorithm for five-axis CNC belt grinders is obtained by solving the machine tool's coordinate transformation matrix. This algorithm converts the tool position file containing the tool axis vector p_n and the tool contact coordinates p_c into NC code containing the motion of each axis. Based on this post-processing algorithm, five-axis post-processing can be implemented, providing an open post-processing platform for retrofitting on-machine measurement modules.

4. Multi-axis CNC belt grinding machine post-processing simulation and experimental verification

The virtual simulation of the completed machine tool is used to simulate the machining of the CNC program obtained through the post-processor conversion, as shown in Figure 23. This simulation environment verifies the correctness of the developed post-processor. A typical sample part of this multi-axis CNC belt grinder is programmed with the process. The post-processor generates a tool position file and the CNC machining program. The verification of the post-processor is divided into three-axis machining verification and five-axis simultaneous machining verification. This study designs the flat parts as the three-axis machining verification object to match the existing tooling fixtures. For the five-axis simultaneous machining verification, this study uses the typical machining parts of this grinder - a certain type of wide chord hollow fan blade as the object.

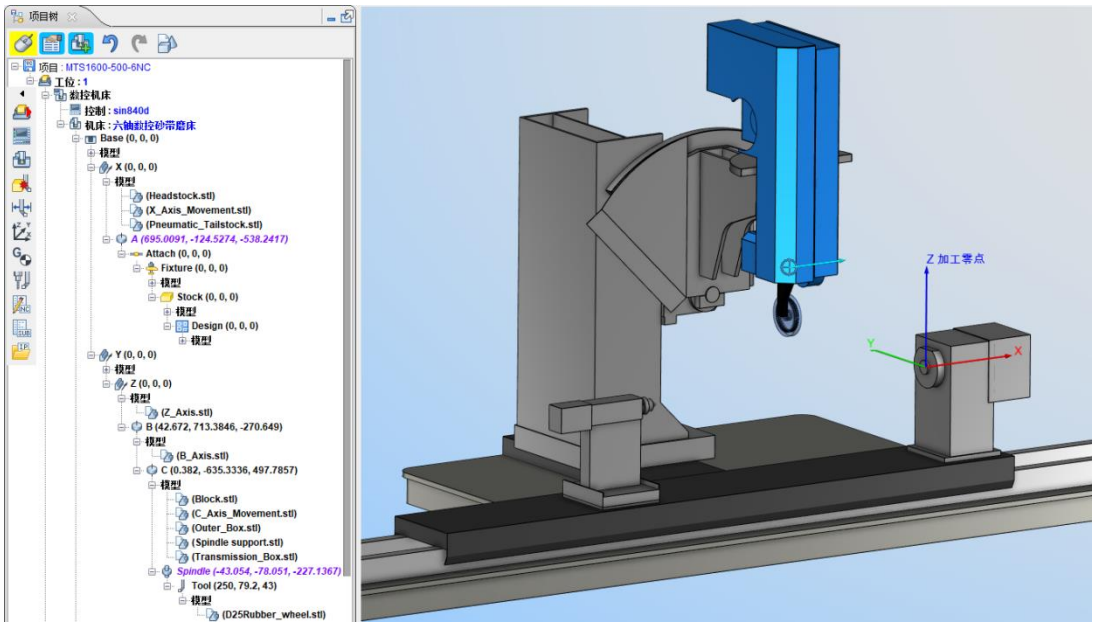

Figure 23 Virtual simulation environment for the MTS1600-500-6NC multi-axis CNC belt grinding machine

4.1 Simulation and experimental verification of CNC programs for machining flat parts

4.1.1 Preparation of jigs and models for flat parts

The simulation is for better experimental verification. So, from the actual experiment perspective, the simulation designs the flat parts and builds its geometrical model based on the dimensions of the existing jigs and fixtures in the workshop. Figure 24 below shows the existing tooling fixture for flat parts in the workshop. The key dimensions of its right side fixture are shown in Figure 25 below, with fixture slot width W=90mm, slot depth D=20mm, and slot spacing H=8mm.

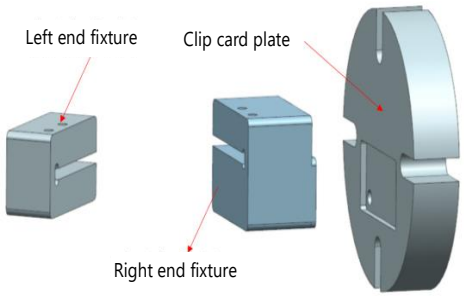

Figure 24 Schematic diagram of a tooling fixture for flat parts

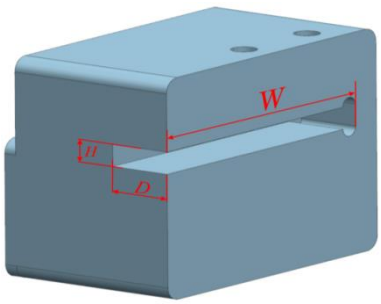

Figure 25 Schematic diagram of the right end fixture dimensions

According to the dimensions of the fixture to establish the size of 400mm×100mm×6mm flat parts geometry model, and in UG to complete the

assembly, as shown in Figure 26, where the red arrow points to the top clamping and screw clamping. Create a blank model with dimensions of 400mm×100mm×7.5 mm and import the overall model into VERICUT.

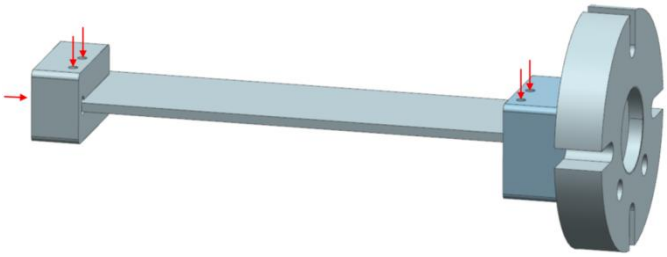

Figure 26 Flat parts and fixtures

4.1.2 Generation of grinding NC programs

In the UG machining module, plane milling is selected instead of grinding for the path planning of the grinding toolpath. As the width of the abrasive belt wheel is 25 mm, a flat-bottomed milling cutter with a diameter of 25 mm is selected instead. The machining step is set to 10 mm. The cutting mode is selected as "reciprocating" according to the actual position of the grinding machine, and the part allowance is set to 0.5 mm. The tool center point is programmed to obtain the grinding toolpath, as shown in Figure 27.

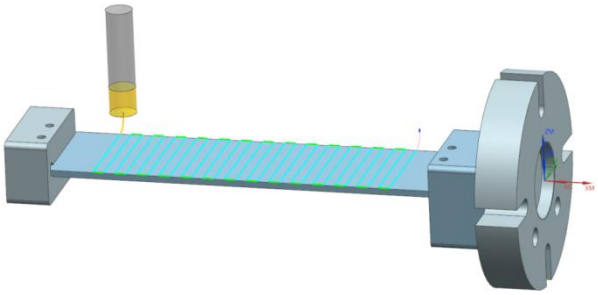

Figure 27 Toolpath for grinding flat parts

After confirming the correctness of the toolpath, it is time to print out the tool position file and use the post-processor developed in Chapter 3 for post-processing to convert the tool position file to an NC program, as shown in Figure 28.

```
TOOL PATH/平板件测试,TOOL,代砂轮
TLDATA/MILL,25.0000,0.0000,75.0000,0.0000,0.0000
MSYS/226.8083,392.8435,0.0000,1.0000000,0.0000000,0.0000000,
$$ centerline data
PAINT/PATH
PAINT/SPEED,10
PAINT/COLOR,186
RAPID
GOTO/-416.0000,70.5000,16.5300,0.0000000,0.0000000,1.0000000
PAINT/COLOR,211
RAPID
GOTO/-416.0000,70.5000,13.0000
PAINT/COLOR,42
FEDRAT/MMPM,250.0000
GOTO/-416.0000,70.3931,11.3684
GOTO/-416.0000,70.0741,9.7648
GOTO/-416.0000,69.5485,8.2165
GOTO/-416.0000,68.8253,6.7500
GOTO/-416.0000,67.9169,5.3905
GOTO/-416.0000,66.8388,4.1612
GOTO/-416.0000,65.6095,3.0831
GOTO/-416.0000,64.2500,2.1747
GOTO/-416.0000,62.7835,1.4515
GOTO/-416.0000,61.2352,0.9259
GOTO/-416.0000,59.6316,0.6069
GOTO/-416.0000,58.0000,0.5000
```

(a) File for flat grinding tool positions

```
; PROGRAM NAME: GRINDING_PRESURE
N100 if $a_in[5]==1 gotof wzw
N110 if $a_in[6]==1 gotof grst
N120 R32=15000  ; EILGANG
N130 G01 B0 F5000
T1
M6
S3000
N140 G01 Z640. F=R32
N150 B0 C0
N160 G642  U1030
N170 SOFT
N180 G01 B0  A=DC(0)
N190 H1=3000 F4980 S3013 M20
N200 M08
N210 M04
N220 G04 F3.0
X-459.000 Y-8.807 Z361.368 B0.000 A=DC(0.000)
X-459.000 Y-9.126 Z359.765 B0.000 A=DC(0.000)
X-459.000 Y-9.651 Z358.216 B0.000 A=DC(0.000)
X-459.000 Y-10.375 Z356.750 B0.000 A=DC(0.000)
X-459.000 Y-11.283 Z355.390 B0.000 A=DC(0.000)
X-459.000 Y-12.361 Z354.161 B0.000 A=DC(0.000)
X-459.000 Y-13.591 Z353.083 B0.000 A=DC(0.000)
X-459.000 Y-14.950 Z352.175 B0.000 A=DC(0.000)
X-459.000 Y-16.417 Z351.452 B0.000 A=DC(0.000)
X-459.000 Y-17.965 Z350.926 B0.000 A=DC(0.000)
X-459.000 Y-19.568 Z350.607 B0.000 A=DC(0.000)
```

(b) NC program for flat grinding

Figure 28 Generating a NC program for flat grinding

4.1.3 Reading the machining code to perform a grinding simulation

The design model of the flat part and the blank model are imported into VERICUT, and the converted NC program is read for virtual simulation machining, the simulation results are shown in Figure 29. Figure 29(a) shows the completion of the virtual simulation environment for the flat part. Figure 29(b) shows the start of the virtual simulation for the flat part. From Figure 29(c), it can be seen that during the simulation process of the flat part, no interference or overcutting occurs between the grinding belt wheel and tool holder and the workpiece being machined. The grinding processing area is consistent with the setting, and the grinding toolpath trajectory is consistent with the setting; during the grinding simulation process, no problems such as machine overtravel, interference, and collision occur. During the grinding simulation, no problems such as overtravel or collision occurred. In summary, the results of the virtual simulation show the correctness of the post-processor during the three-coordinate conversion and the correctness of the virtual simulation environment during the three-axis machining.

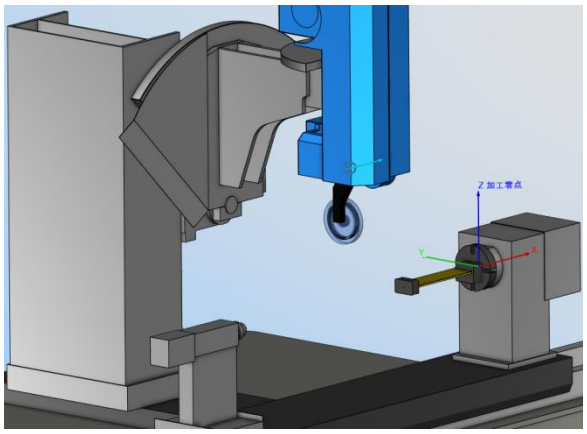

(a) Completed diagram of the simulation environment preparation

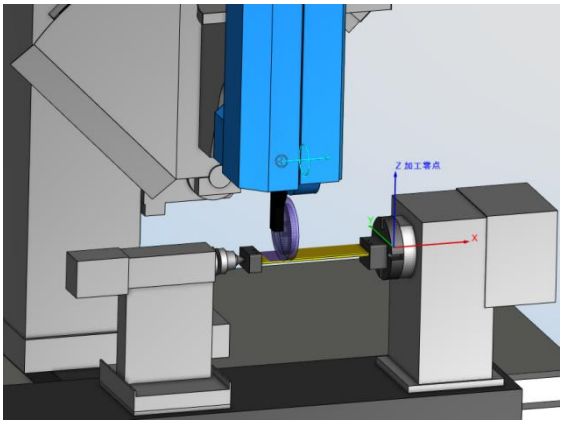

(b) Virtual simulation start diagram

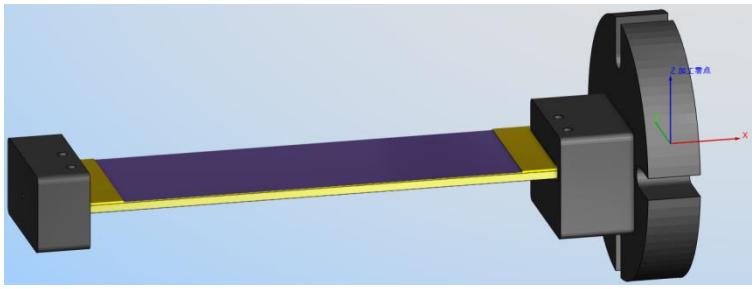

(c) End view of the flat part grinding simulation

Figure 29 Virtual simulation machining of flat parts

4.1.4 Experimental verification of flat pieces

The flat part is clamped onto the grinding machine, and the machining program is imported into the machine controller. As shown in figure 30, the preparation is complete, and the grinding process can begin.

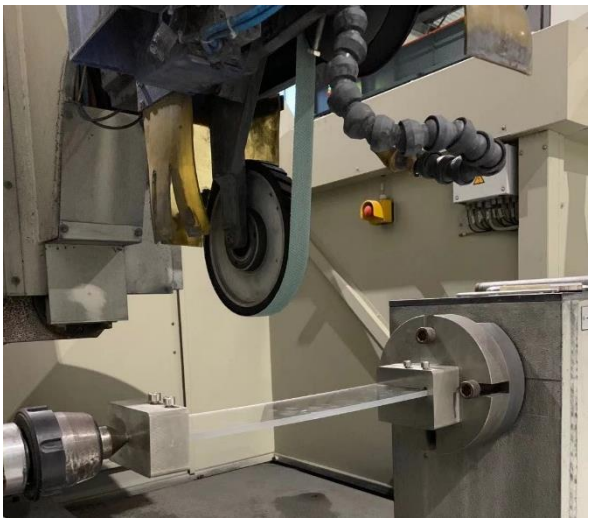

Figure 30 Clamping of flat parts completed

There was no interference with overcutting during the grinding process and no alarms on the travel of the motion axes. The machine completed the grinding process of the flat plate parts completely. During the grinding process, the flat plate made of Plexiglas was prone to bending due to its low rigidity. The grinding depth in the Z-direction could not be guaranteed. This error was due to the nature of the material and did not represent an error in the post-processor. The completed flat piece is shown in Figure 31. The grinding process area is measured to be consistent with the set area, and the grinding path is consistent with the planned path. The experimental results verify the correctness of the post-processor developed by the derivation for three-axis grinding processing.

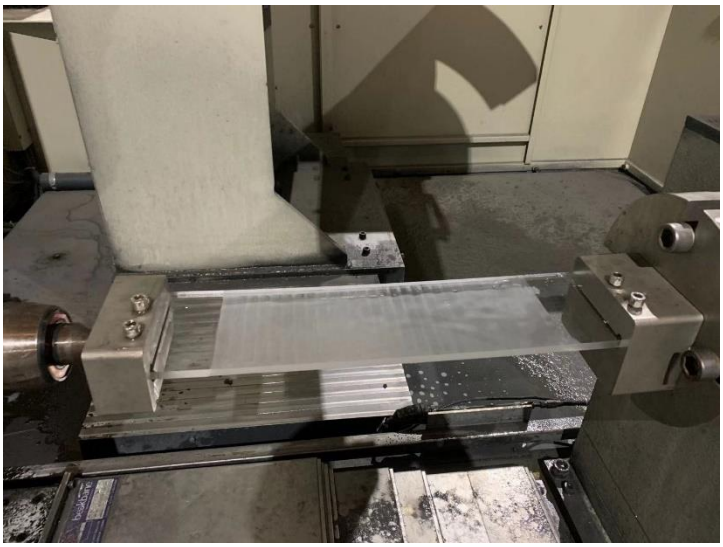

Figure 31 Finished grinding of flat parts

4.2 Wide chord hollow fan blade CNC program simulation and experimental verification

Flat parts are machined in three axes,the results of the flat part grinding simulation can partially verify the correctness of the derived post-processing and the virtual simulation environment built.In order to further validate the correctness of the post-processing and virtual simulation environment, this CNC belt grinding machine will be used to validate the 5-axis machining of a wide chord hollow fan blade, a commonly machined part.

The design model of a wide chord hollow fan blade was assembled with the blank model and its special fixture. A variable profile milling process was created in NX using the mill multi-axis type to program the blade back machining process. The grinding toolpath trajectory for the leaf back is shown in Figure 32. After

confirming and generating the tool position file, the post-processor generates the CNC machining program for the leaf back grinding.

Figure 32 Leaf back grinding toolpath trajectory

Similar to the previous steps, this part of the work exports the completed fixture and blade design model and blank model in UG as stl format and selects the corresponding location in the component tree. Then import the model into VERICUT and add the NC program obtained after the post-processor conversion to VERICUT to start the simulation. The virtual simulation of the grinding of a leaf back is shown in Figure 33. During the simulation, there is no interference or overcutting between the grinding belt wheel and the machined workpiece, and the axes of motion do not exceed their travel. The results of the virtual simulation machining of the leaf backs are shown in Figure 34, which shows that the CNC program can complete the grinding of the leaf backs correctly, proving the correctness of the developed post-processor and the virtual simulation environment of the machine tool.

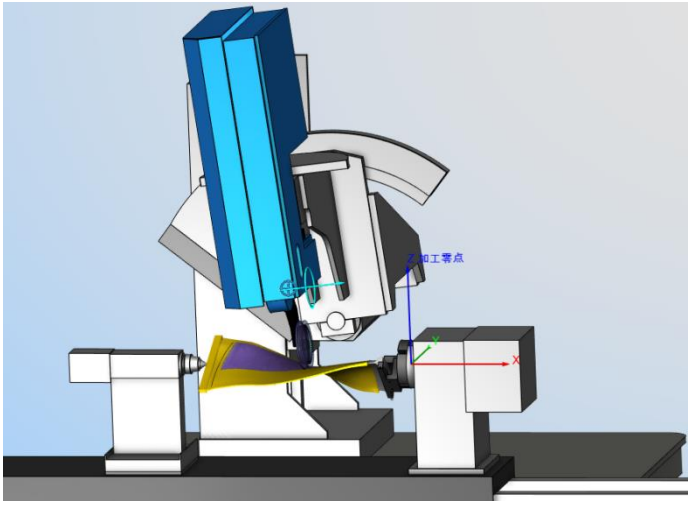

Figure 33 Virtual simulation of the grinding process in progress

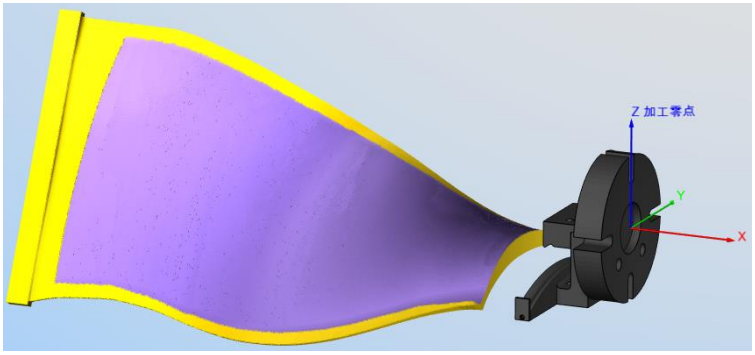

Figure 34 Simulation results of leaf back grinding

To further verify the correctness of the post-processor, the wide chord hollow fan blade, a commonly machined part of this CNC belt grinder, will be used as an experimental verification object for 5-axis machining. The same machine and abrasives are used for the grinding of flat parts, namely the MTS1600-500-6NC CNC belt grinder and 3M™ Trizact™ 363FC abrasive belts in size 25×3500 (width (mm)×circumference (mm)) with a grit of A160.

In order to avoid damage to the machine or the blade due to unknown errors, this experimental verification will use a fan blade that was scrapped in the previous process to reduce the damage. The blade was scrapped due to a pitted dent in the upper left corner of the back of the blade caused by improper operation in the previous process, which had no effect on the overall strength of the blade during grinding and therefore had no impact on the experimental verification. The NC program is the post-processor generated machining program used in the simulation of the machining of the leaf back in chapter 4 above. The fan blade is clamped onto the grinding machine, and the corresponding machining program is imported into the machine controller. As shown in Figure 35, the preparation is complete, and the grinding process can begin.

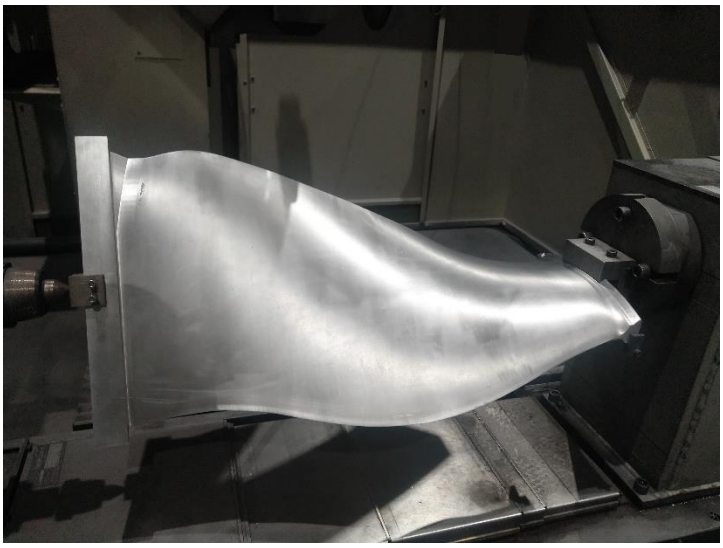

Figure 35 Fan blade clamping completed

Figure 36 shows the overall appearance of the completed grinding of the fan blade backside, and Figure 37 shows the partial details of the completed grinding of the fan blade backside. The experimental results show that the NC program generated by the post-processor can run correctly after being read by the machine tool, the grinding area is consistent with the setting, the machining path is consistent with the planning, and the obtained blade back grinding results are consistent with expectations. The results show that the post-processor developed for this multi-axis CNC belt grinding machine generates the CNC program accurately and without errors and demonstrates the grinding machine's correctness from geometric modeling to component assembly and then to the virtual simulation environment.

Figure 36 Overall view of the completed leaf back grinding

Figure 37 Partial detail of the completed leaf back grinding

5 Conclusion

Multi-axis CNC belt grinding machines are widely used in blade processing and extensively improve the efficiency and accuracy of blade processing. However, the measurement of the blade is still in the manual hand-held measurement stage. There is an urgent need to introduce digital intelligent means to improve. Complete the grinding machine's upgrade for grinding processing and measurement requires reconfiguring the machine's post-processing system. In order to solve this problem, this paper establishes an accurate geometric assembly model of the corresponding multi-axis CNC belt grinding machine based on the machine tool itself. The assembly model lays the foundation for the subsequent reconstruction of the post-processing of the grinding machine and the construction of a virtual simulation environment for the grinding machine.

Based on the geometric assembly model of the CNC belt grinding machine, an auxiliary coordinate system is established with the definition of the initial position of the machine's axes of motion. The overall kinematic chain of the machine is constructed from the machine table group. The machine tool group and the machine's origin offset are determined by deriving the co-ordinate transformation matrix. On the basis of the kinematic chain of the machine tool, this paper derives a coordinate transformation matrix, obtains a post-processing algorithm for the grinding machine, constructs a post-processing coordinate conversion function, and develops a post-processing module based on the kinematic chain of the machine tool. This paper establishes and validates a virtual simulation environment for the grinding machine, then uses a flat part and a wide chord hollow fan blade model as simulation objects to verify the post-processor and machine geometry assembly models' correctness and completes experimental verification with this blade as the object. The work in this paper also provides the basis for the subsequent upgrade of this grinding machine with an on-machine measurement system.

Funding

The research work of this paper is supported by the common technology of "Intelligent manufacturing cell technology of engine hollow blades" (Project No.: 41423010701).

Author Information

- Affiliations

School of Mechatronic Engineering, Xi’an Technological University, Xi’an 700021, Shaanxi, China

Hu Qiao, Zhenxing Wei, Ruixiang Deng and Tianhang Xu

College of Mechanical and Electrical Engineering, Shaanxi University of Science and Technology, Xi’an 710021, Shaanxi, China

Ying Xiang

- Contributions

Hu Qiao and Ying Xiang proposed and developed the concepts related to the study. Hu Qiao contributed to study of post-processing algorithm for multi-axis CNC belt grinder; Zhenxing Wei contributed to modeling and assembly of multi-axis CNC belt grinding machine; Ruixiang Deng contributed to experimental verification and analysis; Tianhang Xu contributed to analysis and manuscript preparation.

- Corresponding Author

Correspondence to Ying Xiang

Declarations

- Conflict of interest

The authors declare no competing interests.

- Ethics approval

The authors declare that this manuscript was not submitted to more than one journal for simultaneous consideration. Also, the submitted work is original and not has been published elsewhere in any form or language.

- Consent to participate and publish

The authors declare that they participated in this paper willingly and the authors declare to consent to the publication of this paper.

References

[1]Yang Yanfeng. Marine propeller surface modeling and five-axis CNC machining tool planning [D]. Dalian University of Technology, 2005.https://doi.org/10.7666/d.y687711.

[2]Leont’ ev M K, Davydov A V, Degtyarev S A, et al. To simulation of fan blade out for a high bypass ratio engine[J]. Russian Aeronautics (Iz VUZ),2014,57(02):27-31. https://doi.org/10.3103/S106879981402007X.
[3]Huang Yun,Huang Zhi. Principles of abrasive belt grinding and its applications [M]. Chongqing: Chongqing University Press, 2009.https://doi.org/10.7666/d.y687711.CNKI:SUN: JXGR.0.2008-24-018.
[4]Wang, Tingting, Zou Lai, Wan Qinghong, et al. A high-precision prediction model of surface roughness in abrasive belt flexible grinding of aero-engine blade[J]. Journal of Manufacturing Processes,2021,66:364-375. https://doi.org/10.1016/j.jmapro.2021.04.002.
[5]Cui Haijun, Zhang Mingqi. Current status and development trend of aero-engine blade polishing technology[J]. Aviation manufacturing technology,2015(11):128-131. https://doi.org/10.16080/j.issn1671-833x.2015.11.128.
[6]Deng Ruixiang, Qiao Hu, An Jiaxiang, et al. Overview on Abrasive Belt Grinding for Complex Surface[C]// Proceedings of the 2019 International Conference on Precision Machining, Non-Traditional Machining and Intelligent Manufacturing (PNTIM 2019), Atlantis Press,2019:66-70.
[7]Cao Xinhang. Research on workpiece adaptive machining technology based on on-machine measurement[D]. Nanjing University of Aeronautics and Astronautics, 2020. https://doi.org/10.27239/d.cnki.gnhhu.2020.000594.
[8]Zhou X., Zhang D., Wu B. H., et al. Generalized method for post-processing of non-orthogonal dual rotary table 5-axis machine tools[J]. Journal of Mechanical Engineering,2014,50(15):198-204. https://doi.org/10.3901/JME.2014.15.198.
[9]Qiu Zhoujingzi. Research on the post-processing technology of general-purpose double pendulum head five-axis CNC machine tools[D]. Harbin Institute of Technology, 2014. https://doi.org/CNKI:CDMD:2.1014.084706.
[10]My C A, Bohez Erik L J. A novel differential kinematics model to compare the kinematic performances of 5-axis CNC machines[J]. International Journal of Mechanical Sciences,2019,163:105-117. https://doi.org/10.1016/j.ijmecsci.2019.105117.
[11]He Yaoxiong, Xu Qihe, Zhou Yanhong. Kinematic modeling and solution of an arbitrary structure CNC machine tool mechanism[J]. Journal of Mechanical Engineering,2002(10):31-36. https://doi.org/10.3321/j.issn:0577-6686.2002.10.008.
[12]Qingchun T , Shaohui Y , Fengjun C, et al. Development of a postprocessor for head tilting-head rotation type five-axis machine tool with double limit rotation axis[J]. International Journal of Advanced Manufacturing Technology, 2018, 97. https://doi.org/10.1007/s00170-018-2195-3.
[13]Zuo Xiaoming,Wu Haibing,Chen Xiaogang. Post-processing and simulation verification of five-axis positioning milling on a non-orthogonal dual rotary table machining centre[J]. Mechanical Science and Technology,2012,31(01):154-158+162. https://doi.org/10.13433/j.cnki.1003-8728.2012.01.009.
[14]So B S , Jung Y H. Inverse Kinematics for Five-axis Machines Using Orthogonal Kinematics Chain[J]. 2008.
[15]Boz Y , Lazoglu I. A postprocessor for table-tilting type five-axis machine tool based on generalized kinematics with variable feedrate implementation[J]. International Journal of

Advanced Manufacturing Technology, 2013, 66(9-12):1285-1293. https://doi.org/10.1007/s00170-012-4406-7.
[16]Tutunea-Fatan O R , Feng H Y. Configuration analysis of five-axis machine tools using a generic kinematic model[J]. International Journal of Machine Tools & Manufacture, 2004, 44(11):1235-1243. https://doi.org/10.1016/j.ijmachtools.2004.03.009.
[17] Zhang Hong. Five-axis machine tool classification kinematic modeling and post-processing verification[J]. Manufacturing Technology and Machine Tools,2019(04):180-183. https://doi.org/10.19287/j.cnki.1005-2402.2019.04.036.
[18]SøRby K. Inverse kinematics of five-axis machines near singular configurations[J]. International Journal of Machine Tools & Manufacture, 2007, 47(2):299-306. https://doi.org/10.1016/j.ijmachtools.2006.03.011.
[19]Sun K , Ni Y , Wang H , et al. Post-processing and simulation of novel five-axis hybrid machine tool[J]. Computer Integrated Manufacturing Systems, 2016. https://doi.org/10.13196/j.cims.2016.01.026.
[20]Yang J , Altintas Y. Generalized kinematics of five-axis serial machines with non-singular tool path generation[J]. International Journal of Machine Tools & Manufacture, 2013, 75:119-132. https://doi.org/10.1016/j.ijmachtools.2013.09.002.
[21]Yang J , Ding H , Zhao H , et al. A generalized online estimation algorithm of multi-axis contouring errors for CNC machine tools with rotary axes[J]. International Journal of Advanced Manufacturing Technology, 2016, 84(5-8):1239-1251. https://doi.org/10.1007/s00170-015-7783-x.
[22]Zhou X Y, Liu Z L, Li M Y,, et al. Post-processor development of a five-axis machine tool with optimization tool radius compensation[J]. International Journal of Advanced Manufacturing Technology, 2017, 88(5-8):1505-1522. https://doi.org/10.1007/s00170-016-8801-3.
[23]Luo, Ming, Zhang, et al. Kinematic analysis and feedrate optimization in six-axis NC abrasive belt grinding of blades[J]. International Journal of Advanced Manufacturing Technology, 2015. https://doi.org/10.1007/s00170-015-6824-9.
[24]Zhao Dan, Bi Yunbo, Ke Yinglin. Kinematic modeling and inverse kinematics solution of a new six-axis machine tool for oval hole drilling in aircraft wing assembly[J]. The International Journal of Advanced Manufacturing Technology,2018,96(05):2231 – 2243. https://doi.org/10.1007/s00170-018-1785-4.
[25]Tang Q C , Yin S H , Zhang G H , et al. Post-processor development for a turning and milling composite machine tool[J]. International Journal of Advanced Manufacturing Technology, 2018,95:131 – 141. https://doi.org/10.1007/s00170-017-1139-7.
[26]Zhao D, Bi Y B, Ke Y L. Kinematic modeling and base frame calibration of a dual-machine-based drilling and riveting system for aircraft panel assembly[J]. International Journal of Advanced Manufacturing Technology, 2018, 94:1873 – 1884. https://doi.org/10.1007/s00170-017-0982-x.
[27]Yuen A , Altintas Y . Trajectory generation and control of a 9 axis CNC micromachining center[J]. CIRP Annals - Manufacturing Technology, 2016:349-352. https://doi.org/10.1016/j.cirp.2016.04.098.

[28]Song D , Xue F , Zhang J , et al. Postprocessor algorithm and feedrate optimization for nine-axis milling machine tool with twin cutters[J]. International Journal of Advanced Manufacturing Technology, 2019, 103(1). https://doi.org/10.1007/s00170-019-03661-x.
[29]Zhou Feng, Zhang Zixu, Wu Chang, et al. Optimization of Numerical Control Program and Machining Simulation Based on VERICUT[J]. Journal of Shanghai Jiaotong University (Science),2019,24(06):763-768. https://doi.org/10.1007/s12204-019-2109-z.
[31]Xiong Yi, Wang Zhe, Tang Jiansheng, et al. Research status and development trend of CNC machining simulation system[J]. Manufacturing Technology and Machine Tools,2011(12):71-75. https://doi.org/10.3969/j.issn.1005-2402.2011.12.022.
[31]Ren Jinggang. Status and trends of the development of CNC machining simulation technology[J]. Aviation manufacturing technology,2016(05):62-66. https://doi.org/10.16080/j.issn1671-833x.2016.05.062.